CONF-771120--20

COMPUTING THE EFFECT OF PLASTIC DEFORMATION OF PIPING ON PRESSURE TRANSIENT PROPAGATION

C. K. Youngdahl and C. A. Kot

MASTER

Prepared for

ASME
American Society of Mechanical Engineers
Atlanta, GA
November 1977

ARGONNE NATIONAL LABORATORY, ARGONNE, ILLINOIS

Operated under Contract W-31-109-Eng-38 for the
U. S. DEPARTMENT OF ENERGY

COMPUTING THE EFFECT OF PLASTIC DEFORMATION OF PIPING ON PRESSURE TRANSIENT PROPAGATION

C. K. Youngdahl and C. A. Kot
Components Technology Division
Argonne National Laboratory
Argonne, Illinois 60439

ABSTRACT

The computer program PTA-1 performs pressure-transient analysis of large piping networks using the one-dimensional method of characteristics applied to a fluid-hammer formulation. The effect of elastic-plastic deformation of piping on pulse propagation is included in the computation. Each pipe is modeled as a series of rings, neglecting axial effects, bending moments, and inertia. The fluid wave speed is a function of pipe deformation and, consequently, of position and time. Comparison with existing experimental data indicate that this simple fluid-structure interaction model gives surprisingly accurate results for both pressure histories in the fluid and strain histories in the piping.

NOMENCLATURE

c = Wave speed in fluid
C^+, C^- = Characteristic curves
D = Pipe diameter
E = Elastic modulus
f = Darcy-Weisback pipe-friction factor
g = $f\,u|u|/2D$, friction term
H = Pipe wall thickness
K = Bulk modulus of fluid
p = Pressure
t = Time
u = Fluid velocity
v = Defined by eq. (13)
x = Axial coordinate along pipe
Δt = Time step
Δx = Axial grid spacing
ϵ = Circumferential strain in pipe
θ = $\Delta t/\Delta x$
ρ = Fluid density
σ = Circumferential stress in pipe

Subscripts

A,B,P,Q,R,S = Grid points (see Fig. 2)

Superscripts

+,- = Values along characteristics

INTRODUCTION

The computer program PTA-1 performs pressure transient analysis of large piping networks using the one-dimensional method of characteristics applied to a fluid-hammer formulation. It is particularly oriented toward the analysis of the effects of a sodium/water reaction on the intermediate heat transport system of a liquid-metal-cooled fast-breeder reactor, but may just as usefully be applied to other pulse sources and other piping systems. The effect of elastic-plastic deformation of piping on pulse propagation is included in the computation since the pressure pulses anticipated from a sodium/water reaction exceed the yield pressure of the thin-walled piping. PTA-1 is capable of treating complex piping networks and includes a variety of junction types. Pipe friction and nonlinear velocity terms are included in the formulation. The program requires a minimum of input data preparation, is designed to be easily used and modified, and has a short running time. PTA-1 is the first in a series of computer programs developed to analyze pressure transients in reactor piping systems; subsequent versions will include the effects on pulse propagation of cavitation, pipe motion, and complex flow components, such as heat exchangers and pumps.

Stainless steel piping is used for the heat transport systems of breeder reactors because of its compatibility with liquid metal coolants. Since operating pressures are low (about 1 MPa (145 psi)), thin-walled large-diameter piping is employed. At operating temperatures the yield pressure of this piping is about 5 MPa (725 psi). Since a sodium/water reaction in a steam generator may produce a pressure pulse of about 10 MPa (1450 psi), a reactor piping system is particularly susceptible to plastic deformation. As shown in a Stanford Research Institute experiment (1), an effect of plastic pipe deformation on a pressure transient is to chop the peak pressure to about the yield pressure of the pipe as the pulse moves down its length.

Various modelings of the effect of pipe deformation on hydraulic transient propagation are conceivable, ranging from a rigid pipe-wall model with no structure-fluid interaction effects to a detailed modeling of dynamic deformations and stresses in the piping and the resultant interactions of the stress waves and pipe vibrations with the fluid motion. The model used here was suggested by Fox and Stepnewski (2) and is essentially the simplest pipe-response model that incorporates some influence of plastic wall deformation on transients in the fluid. It has the advantages of being readily incorporated into standard fluid-hammer analysis procedures (3) and giving results that are conceptually plausible and agree well with available experimental evidence on plastic wall deformation interaction with fluid-transient propagation.

The assumptions involved in this pipe response model include:

- The pipe response is quasi-static, i.e., the pipe deformation is in equilibrium with the fluid pressure, which varies with position and time. This eliminates all waves traveling through the pipe material.

- Bending moments in the pipe wall are neglected, and pipe deformations are not required to be continuous functions of axial position. This implies that the pipe is treated as a series of rings which act independently of each other.

- Axial stresses and strains in the pipe are neglected.

- The pipe wall is thin enough that circumferential stress variations across the thickness can be neglected.

The result of these assumptions on pipe response is that the only influence of pipe deformation on transient propagation in the fluid is through its effect on local wave speed. The wave speed, which is equal to the sound speed in the fluid if wall-deformation effects are neglected, is no longer just a function of fluid properties, but now depends on fluid properties, pipe properties, pipe-deformation history, circumferential stress, and direction of loading. Consequently, it can vary with time and position along the pipe, and provision is made in the computational scheme to accommodate this variation.

The computational procedure used in PTA-1 is the one-dimensional method of characteristics in a fixed time-space grid. In regions where the wave speed is constant (elastic pipe deformation), an explicit solution for fluid velocity and pressure at time $t + \Delta t$ is obtained from values at time t by using interpolation to determine the intersections of the characteristics with the grid. In variable wave-speed regions (plastic pipe deformation), an iterative procedure is employed to use information at both $t + \Delta t$ and t in computing the slopes of the characteristics and their intersections with the grid.

PTA-1 is designed to be easily used and modified. There are no restrictions on pipe and junction numbering schemes or designations of left and right ends of pipes, and the flow network is assembled by the program. Node spacings, fluid properties, pipe material properties, pipe flow areas, friction factors, wave speeds, and junction losses are computed internally. Pipes made of many different materials can be included in the same network; temperature-dependent stress-strain relations for Types 304 and 316 stainless steels are included in the material properties subroutine, as well as arbitrary functional relations for describing other materials. Each type of junction is modeled in a separate subroutine to facilitate modifications and improvements; the junction types include multi-branched tees, pumps, acoustic impedance discontinuities, dummy junctions, closed ends, surge tanks, nonreflecting far ends, rupture disks, and pulse sources.

The basic equations and numerical procedures used in PTA-1 are summarized in the next section. The validation of PTA-1 using the results of recent pipe response experiments performed at Stanford Research Institute (4) is then presented, followed by a discussion of the implications of this validation on the computational modeling of pipe deformation effects on pressure transients.

EQUATIONS

Applying the one-dimensional method-of-characteristics to fluid flow and continuity relations results in equivalent differential equations that involve only total derivatives with respect to time and apply only along characteristic curves; these are (5):

$$\frac{du}{dt} + \frac{1}{\rho c}\frac{dp}{dt} + g(u) = 0 , \qquad (1)$$

which holds along the positive characteristic C^+, given by

$$dx = (u + c)dt , \qquad (2)$$

and

$$\frac{du}{dt} - \frac{1}{\rho c}\frac{dp}{dt} + g(u) = 0 , \qquad (3)$$

which holds along the negative characteristic C^-, given by

$$dx = (u - c)dt . \qquad (4)$$

The local wave speed, including both the effects of fluid compressibility and pipe deformation (2,3), is given by

$$c^2 = \frac{K/\rho}{1 + \frac{KD}{H(\frac{d\sigma}{d\varepsilon} - 2\sigma)}}, \qquad (5)$$

where the stress is related to the fluid pressure through

$$\sigma = \frac{pD}{2H} . \qquad (6)$$

If the pipe is rigid, the second term in the denominator of eq. (5) vanishes and the wave speed becomes the speed of sound in the fluid. If the pipe responds elastically, $d\sigma/d\varepsilon = E$ and, since $E >> 2\sigma$, the wave speed is a constant for the pipe. On the other hand, the wave speed varies with position and time along a plastically deforming pipe; moreover, $d\sigma/d\varepsilon$ and σ depend not only on the current value of p, but also on prior strain history and the sign of dp. If there has been plastic deformation at a pipe cross section followed by elastic unloading (path 123 in Fig. 1), the yield stress, which was originally σ_1, will be increased

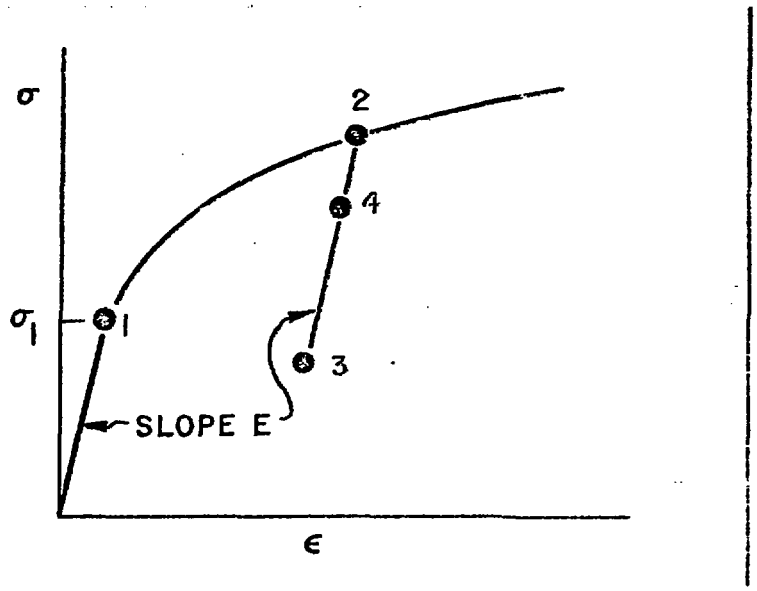

Figure 1. Typical stress-strain relation

by strain hardening to σ_2; stresses such as σ_4, which would have produced plastic deformation originally, will now produce elastic deformation with its correspondingly higher wave speed. If a pipe cross section is deforming plastically (point 2 in Fig. 1), a further pressure increase will produce additional plastic deformation, corresponding to a low wave speed; conversely, a pressure decrease will produce elastic unloading corresponding to a high wave speed. The maximum stress experienced at each axial node point of a plastically deforming pipe is monitored. If the previous maximum stress at a particular point is less than the original yield stress σ_1, the current stress is compared with σ_1 to determine whether the corresponding deformation is elastic or plastic. If the previous maximum stress is σ_2, which is greater than σ_1, the current stress is compared with σ_2 to determine whether the current deformation is elastic or plastic.

If the solution for pressure and fluid velocity is known at a time t_o for every position x along a pipe, the solution at a later time $t_o + \Delta t$ can be found through the relations between du/dt and dp/dt that hold along the characteristic curves (Fig. 2). Expressing eqs. (1) and (3) in finite-difference form for C^+ and C^- characteristics intersecting at point P gives

$$u_P - u_A + \frac{1}{\rho c_A^+}(p_P - p_A) + g(u_A^+)\Delta t = 0 \qquad (7)$$

and

$$u_P - u_B - \frac{1}{\rho c_B^-}(p_P - p_B) + g(u_B^-)\Delta t = 0 , \tag{8}$$

where c_A^+ and u_A^+ are appropriately averaged values of wave speed and fluid velocity along the C^+ characteristic between points A and P, and c_B^- and u_B^- are appropriately averaged values of wave speed and fluid velocity along the C^- characteristic between points B and P.

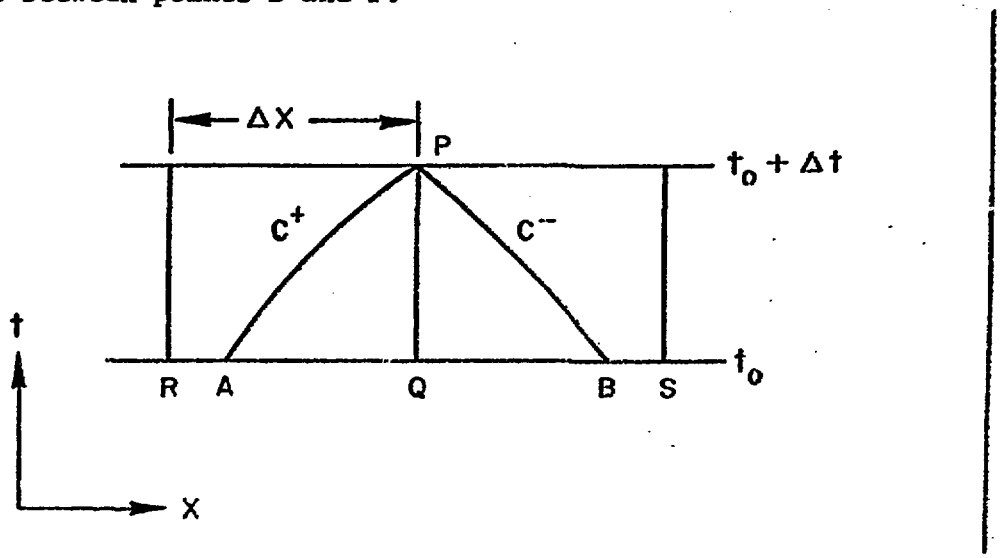

Figure 2. Finite-difference grid

If the pipe is rigid or is deforming elastically, the wave speed is constant along the characteristics. However, the wave speed can vary significantly along the characteristics if the pipe is deforming plastically; for this case, we will take

$$\begin{aligned} c_A^+ &\approx \frac{1}{2}(c_A + c_P) , \\ c_B^- &\approx \frac{1}{2}(c_B + c_P) , \end{aligned} \tag{9}$$

where c_A, c_B, and c_P are the local wave speeds corresponding to conditions at nodes A, B, and P, respectively.

The Courant-Friedrichs-Lewy criterion for convergence and stability of the finite-difference scheme used here requires that the time step Δt and axial grid spacing Δx for a pipe satisfy

$$\Delta x \geq (c + |u|)\Delta t . \tag{10}$$

Since the time step is the same for the entire system and the wave speed varies from pipe to pipe if the pipes deform, it is necessary to initially select Δx for each pipe so as to satisfy the above inequality. For strain-hardening materials, the fluid wave speed corresponding to elastic deformation is greater than that corresponding to plastic deformation; consequently, the former is used in determining Δx. The time step is decreased during the course of the computation if violation of the stability criterion is imminent.

The interpolations required in the fixed time-space grid have two aspects; The locations of the intersections of the characteristics with the constant time line (points A and B of Fig. 2) must be determined; and then values of the desired quantities must be computed at these locations in terms of their values at the grid points. Let v_A^+ be an appropriately averaged value of $u + c$ along the C^+ characteristic through points A and P, and let v_B^- be an appropriately averaged value of $u - c$ along the C^- characteristic through points B and P. For a rigid or elastically deforming pipe, the wave speed is constant along the

characteristics, and, since the fluid velocity is small compared to the wave speed, we can take

$$v_A^+ \approx u_A + c, \quad v_B^- \approx u_B - c \ . \tag{11}$$

Linear interpolation then gives

$$u_A = \frac{u_Q - c(u_Q - u_R)\theta}{1 + (u_Q - u_R)\theta} \ ,$$

$$u_B = \frac{u_Q + c(u_S - u_Q)\theta}{1 + (u_S - u_Q)\theta} \ . \tag{12}$$

For plastically deforming pipe, the wave speed varies significantly along the characteristics. For this case, we will take

$$v_A^+ \approx \frac{1}{2}(u_A + c_A + u_P + c_P) \ ,$$

$$v_B^- \approx \frac{1}{2}(u_B - c_B + u_P - c_P) \ . \tag{13}$$

Since u_P and c_P (which depends on p_P) are unknown at time t_o, an iterative solution is required between interpolated quantities and equations for u_P and p_P given below. In computing c_A and c_B, it is necessary to know the maximum pressures experienced at points A and B up to time t_o; these are interpolated from stored maximum pressures at the node points.

At an interior node, eqs. (7) and (8) can be solved for u_P and p_P to give

$$u_P = [c_A^+(u_A - g_A\Delta t) + c_B^-(u_B - g_B\Delta t) + (p_A - p_B)/\rho]/(c_A^+ + c_B^-),$$

$$p_P = [p_A/c_A^+ + p_B/c_B^- + \rho(u_A - g_A\Delta t - u_B + g_B\Delta t)]c_A^+ c_B^-/(c_A^+ + c_B^-). \tag{14}$$

For rigid or elastic pipe walls, these equations give explicit closed-form relations for u_P and p_P. For plastically deforming pipe walls, c_A^+, c_B^-, and the interpolations for p_A, p_B, u_A, and u_B depend on u_P and p_P. Consequently, an iterative procedure is employed to compute these quantities.

The types of junctions included in PTA-1 are tees, pumps, acoustic impedance discontinuities, dummy junctions, closed ends, constant-pressure surge tanks, nonreflecting far ends, rupture disks, and pressure sources. The governing equations for each of these types of boundary nodes are given in the user's manual for the program (6).

EXPERIMENTAL VALIDATION

Stanford Research Institute has performed a series of experiments (4) to measure the effect of plastic deformation of piping on pulse propagation in one-eighth scale models of typical reactor piping. Four experiments involving plastic deformation were performed. Comparison of the results of one of these tests, FP-E-101, with PTA-1 computations will be discussed here. The qualitative and quantitative agreement between experimental and computed results were equally good for the other three tests, which differed in their piping arrangements.

The test configuration for SRI Experiment FP-E-101 is shown in Fig. 3. A thick-walled steel pipe [3.05 m (10 ft) long, 73 mm (2.87 in.) inside diameter, 4.8 mm (0.188 in.) wall thickness] is connected to a thin-walled

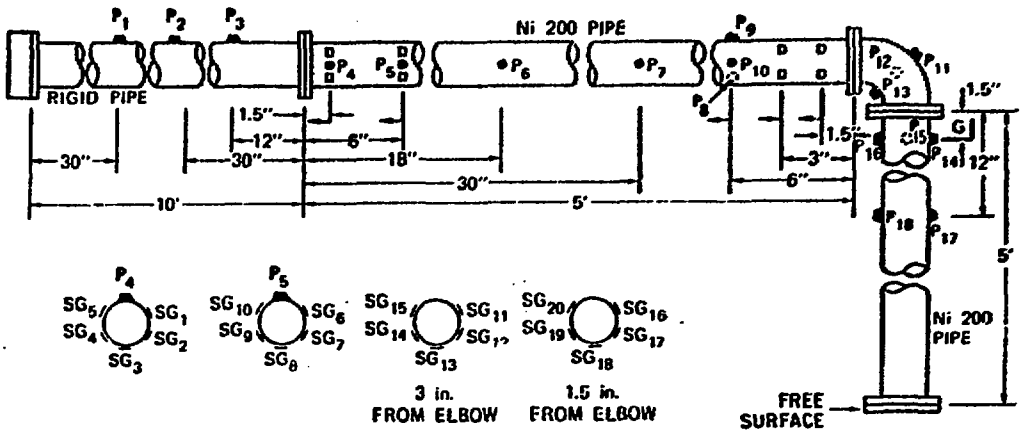

Figure 3. Test configuration for SRI experiment (Reproduced from Romander and Cagliostro (4))

Nickel 200 pipe [1.52 m (5 ft) long, 73 mm (2.87 in.) inside diameter, 1.65 mm (0.065 in.) wall thickness]. The latter is followed by a thick-walled steel elbow and another nickel pipe of the same size as the first. A free surface terminates the system for this test. Nickel 200 was used because its stress-strain curve at room temperature is similar to that of stainless steel at reactor operating temperature. The piping system was filled with water, and all flanges were rigidly fixed to prevent pipe motion. An explosively driven pulse gun at the left end of the system provided an input pulse having a peak pressure of about 14 MPa (2000 psi), a rise time of about 0.2 ms, and a duration of about 3 ms. This pulse was intended to model that of a hypothetical core disruptive accident, but it is also a reasonable representation of a pulse resulting from a hypothetical sodium/water reaction in an LMFBR steam generator. The nickel pipes were deformed plastically by the pulse, but the steel pipe and elbow only deformed elastically. Pressure and strain histories were recorded using pressure gauges P_1-P_{18} and strain gauges SG_1-SG_{20}, located as shown in Fig. 3. Maximum dynamic strains and permanent strains were determined at various axial locations from the strain-time results and checked by post-test measurements. The pressure pulse at gauge 1 (see Fig. 4) was used as the source pulse for the PTA-1 computation.

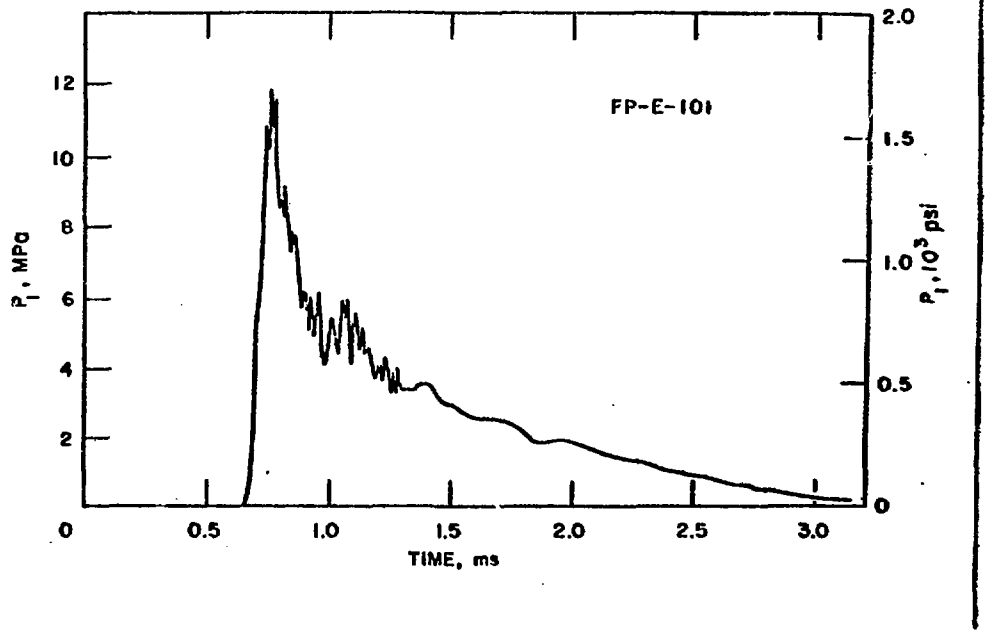

Figure 4. Pressure history $P_1(t)$ used as source pulse in PTA-1 computation

PTA-1 currently models elbows as ordinary straight pipe junctions, and ignores attenuating effects of elbow curvature on pulse propagation. One objective of the Pressure Transient Analysis Techniques Program at ANL is to develop equivalent one-dimensional computational models of flow components for incorporation into the PTA series of codes. (To be a practical design tool, the codes must be basically one-dimensional because of the size and complexity of typical LMFBR heat transport systems.) Consequently, the SRI elbow tests are potentially useful in estimating the magnitude of the attenuating effect of elbow curvature on pulse propagation and in determining the feasibility of developing an equivalent one-dimensional model for three-dimensional pulse propagation around an elbow.

SRI reported negligible circumferential variation of pressure from multiple gauges at and near the elbow. For example, peak pressures measured by gauges P_{11} and P_{13} were 3.279 and 3.289 MPa (475.6 and 477.1 psi), respectively, and the measured pulse shapes were essentially identical. The experimental results indicate that not only is a one-dimensional computational model for an elbow feasible, but that a multidimensional model is not likely to be more accurate, at least for the elbow geometry and pulse characteristics used in the experiment. Since the diameter, wall thickness, and material of the elbow differ from those of the nickel pipes connected to it, there is an impedance discontinuity at the elbow that affects the transmitted pulse in addition to the elbow-curvature effect. Therefore, to isolate the effect of elbow curvature on pulse attenuation, the elbow was modeled in PTA-1 as a section of straight pipe having the same diameter, wall thickness, and mean length as the elbow.

Figures 5 and 6 compare experimental results (curves) and PTA-1 computations (small circles) at pressure gauges P_2 and P_3 in the stiff steel pipe. A rarefaction wave is reflected back from the junction with the plastically deforming nickel pipe, causing cavitation in the steel pipe; this is indicated both by the bottoming out of the experimental measurements and by the negative computed pressures. A parallel computation which considered only elastic deformation of the nickel piping did not predict any negative pressures in the steel pipe. Consequently, an indirect effect of plastic deformation of a pipe on pulse propagation is the unexpected, but experimentally verified, occurrence of cavitation in another pipe, which is itself only deforming elastically.

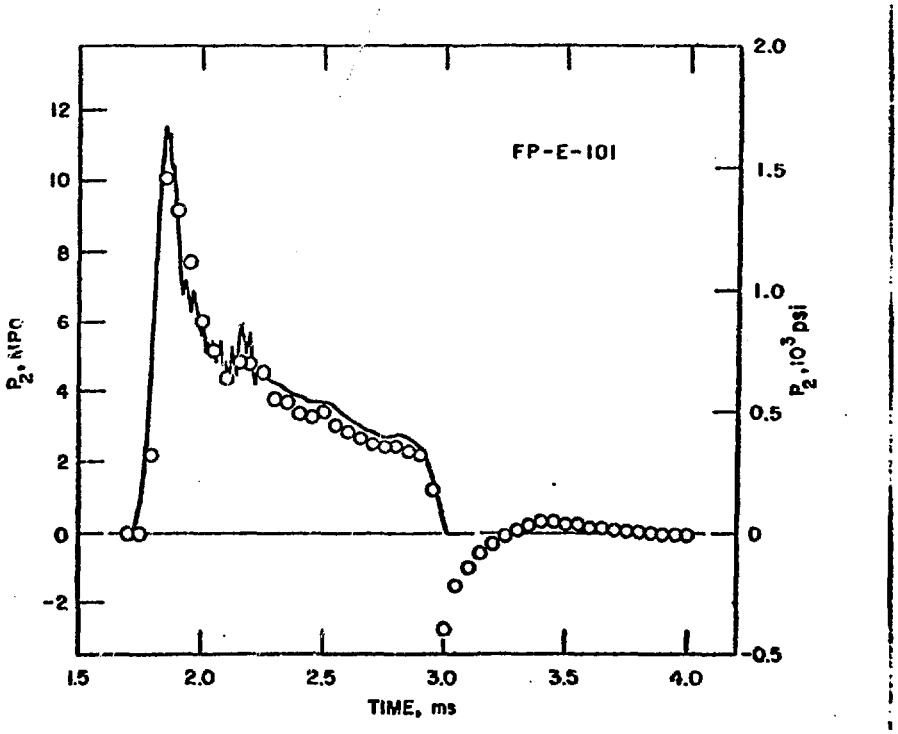

Figure 5. Experimental and computed pressure histories $P_2(t)$

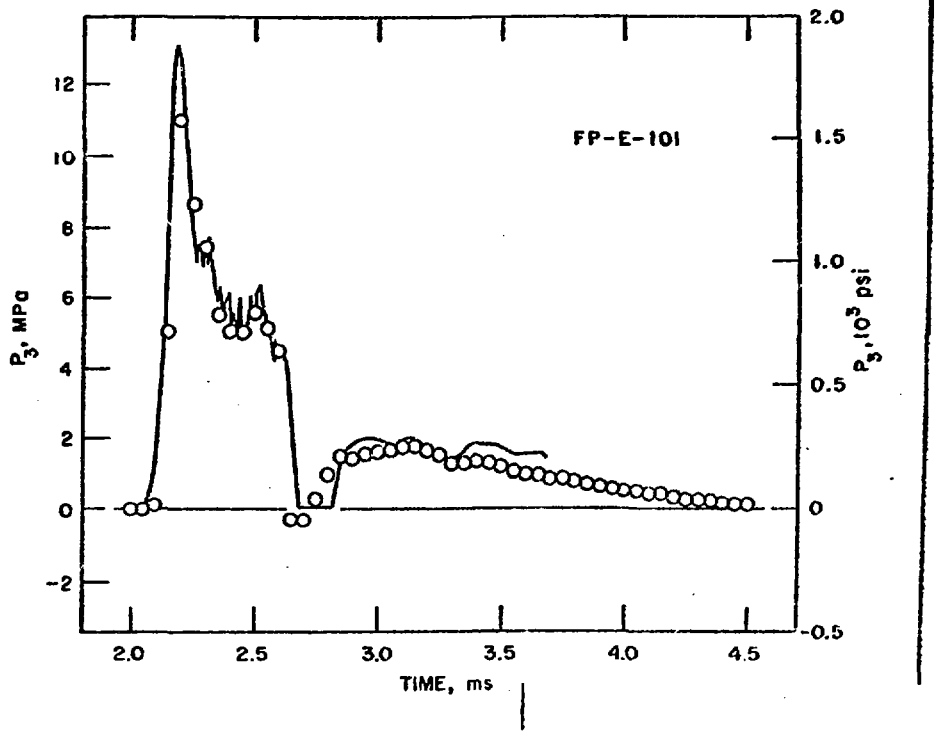

Figure 6. Experimental and computed pressure histories $P_3(t)$

Figures 7-10 show comparisons between experiment and computation at pressure gauge locations in the first nickel pipe. Without plastic deformation, the pressure peak of about 12 MPa (1750 psi) shown in Figs. 4-6 would travel essentially undiminished through the system. Plastic deformation eventually chops this peak to the yield pressure of the piping, about 3.5 MPa (500 psi), and spreads out the pulse. The agreement between computation and experiment is quite good, except at gauge 4; this gauge is close to a heavy flange, which may have contributed to the noise in the experimental results and the computed overprediction of pressure. However, the agreement between measured and calculated strain histories at this location is excellent.

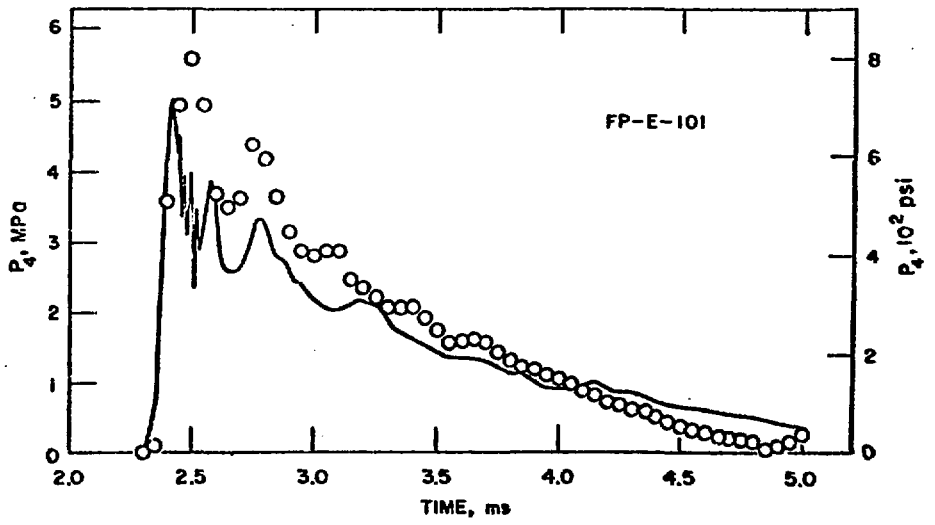

Figure 7. Experimental and computed pressure histories $P_4(t)$

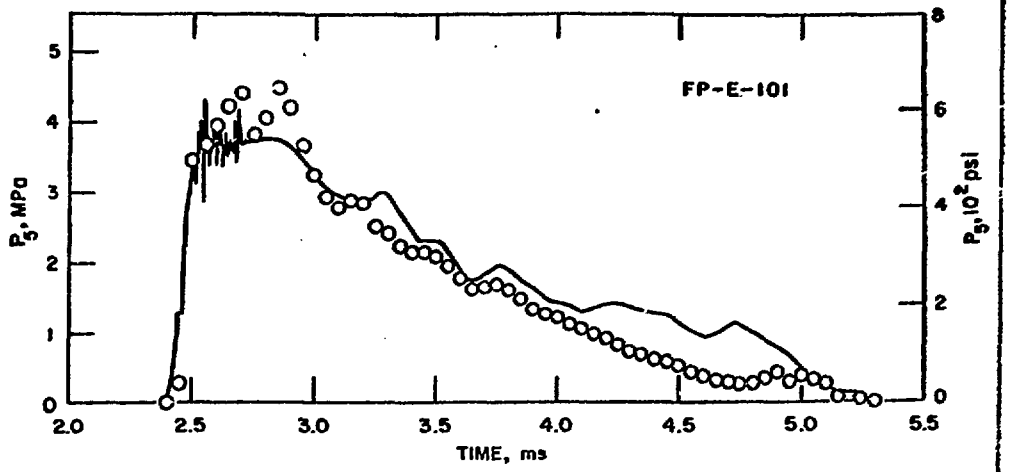

Figure 8. Experimental and computed pressure histories $P_5(t)$

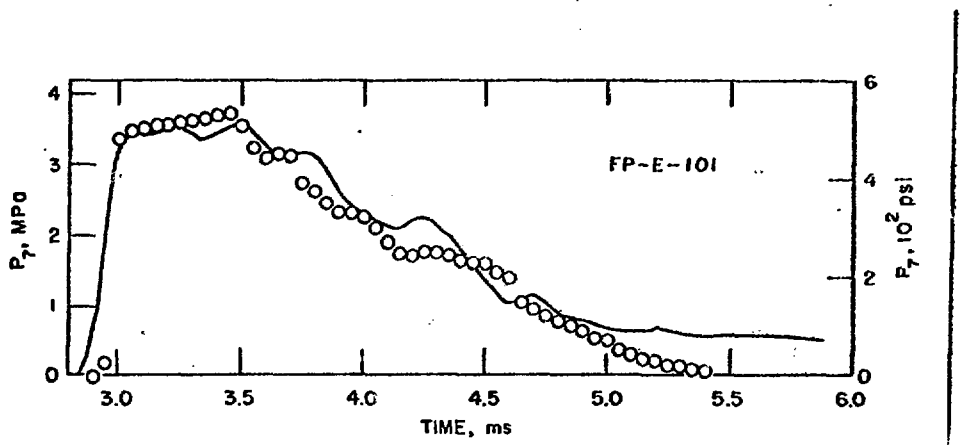

Figure 9. Experimental and computed pressure histories $P_7(t)$

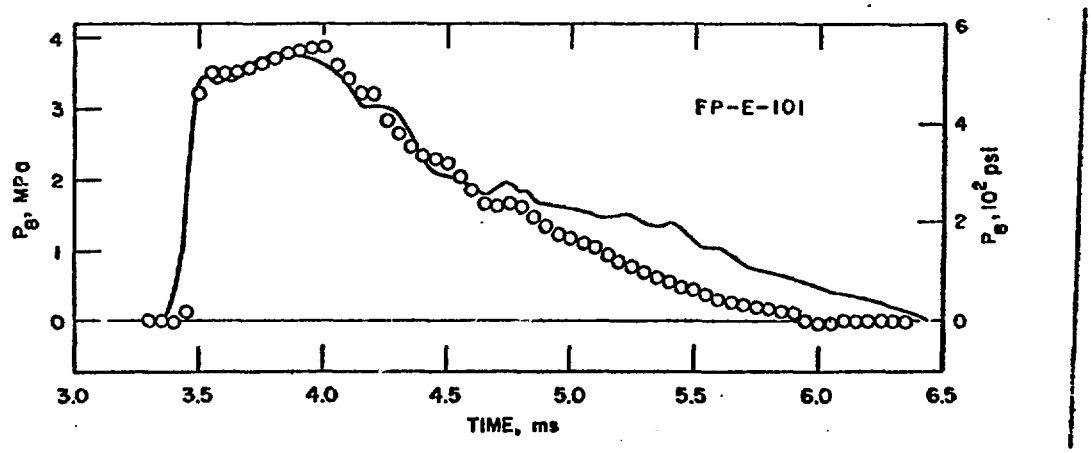

Figure 10. Experimental and computed pressure histories $P_8(t)$

The computed peak pressure at the midsection of the elbow is 0.5 MPa (75 psi) greater than the measured value (see Fig. 11). This disparity is also evident at gauge 16, just beyond the elbow (see Fig. 12). However, at

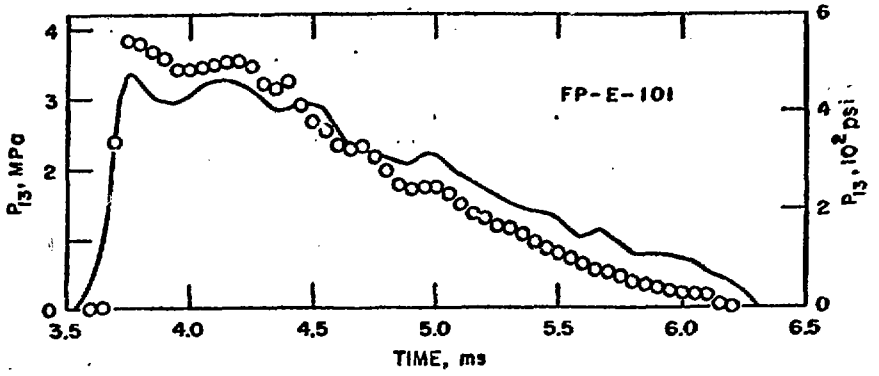

Figure 11. Experimental and computed pressure histories $P_{13}(t)$

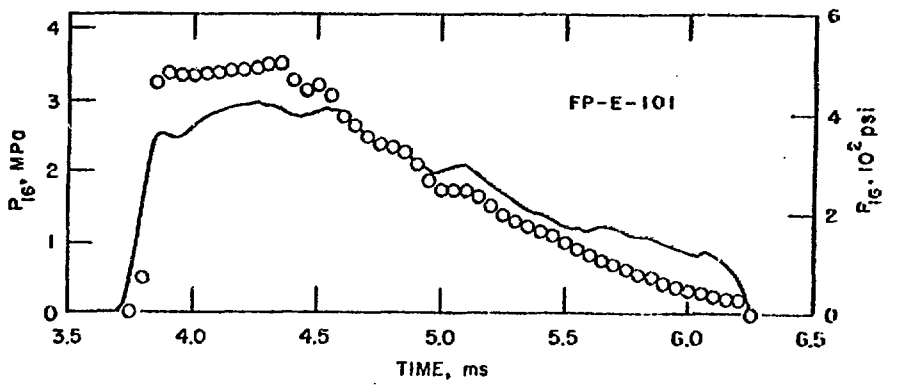

Figure 12. Experimental and computed pressure histories $P_{16}(t)$

gauge 18, which is 0.15 m (6 in.) beyond the elbow, there is excellent agreement between computation and experiment, as shown in Fig. 13. The effect of elbow curvature on pulse propagation appears to be localized near the elbow; moreover, the discrepancy in peak pressure at the elbow may not be associated with elbow curvature, but may be a result of the slight ovality ($\sim$ 2%) of the elbow cross section. It should be emphasized that plastic deformation chops off pressure peaks and thus may be masking any effect of elbow curvature.

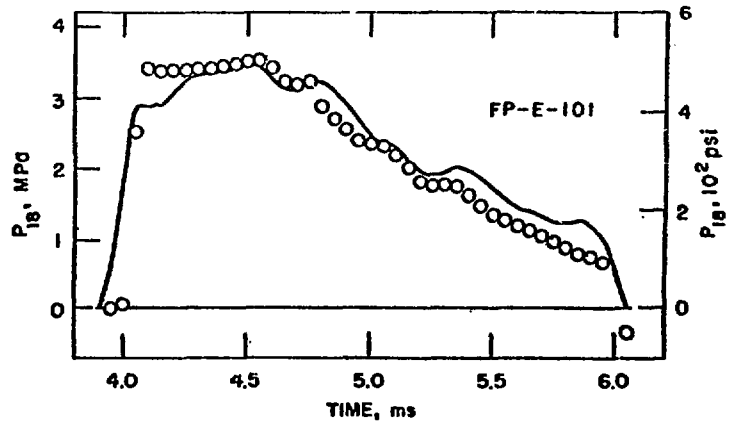

Figure 13. Experimental and computed pressure histories $P_{18}(t)$

The pipe-plasticity model used in PTA-1 was devised to incorporate the effect of plastic deformation of the piping on pressure-pulse propagation in the fluid. The model was not intended or expected to also predict strain histories in the piping with any quantitative or qualitative accuracy because of the rather crude assumptions made with regard to plastic deformation. Consequently, although all information required to calculate strain histories was computed in PTA-1, the strains were not explicitly computed in the original version of the program (6). Since extensive strain data was obtained in the SRI experiments, a subroutine was added to PTA-1 to compute circumferential strain in the piping. The agreement obtained between computation and experiment was surprisingly good. At all strain gauge locations (see Fig. 3), the computed strain histories match the experimental results well with respect to general shape, location and duration of initial rises, location of peaks, and decay amplitudes; quantitatively they provide a good prediction of the mean of the five strain-time measurements at each axial location.

The comparison of computed and experimental values of maximum dynamic strain as a function of axial location for Experiment FP-E-101 is shown in Fig. 14. The curve is the computed strain distribution, the bars show the spread in the readings of the five strain gauges at each axial location where measurements were made, and the dots indicate the average of the five values.

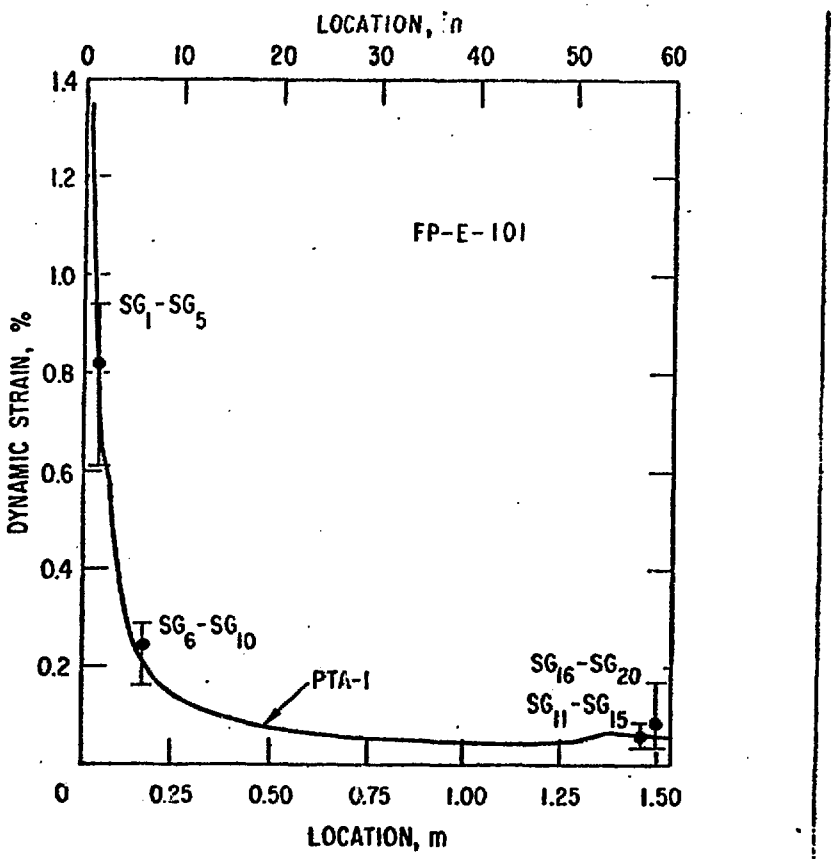

Figure 14. Experimental and computed distribution of maximum dynamic strain in first nickel pipe

A fairly large circumferential variation of strain was measured at each axial location. This was attributed to wall-thickness variations around the circumference; post-test wall-thickness measurements did indeed show that, at a given axial location, the largest strains occurred where the thickness was smallest, and vice versa. In all cases, the computed results are well within the circumferential variation in the experimental measurements. In addition,

post-test measurements of diameter change as a function of axial position give permanent deformation profiles that agree with the computed permanent strain distributions.

CONCLUSIONS

Some conclusions that may be drawn from this study are:

•Plastic deformation of piping typical of reactor heat transport systems can have a significant qualitative and quantitative effect on pressure pulse propagation.

•The simple, one-dimensional computational model incorporated in PTA-1 for predicting plastic-deformation effects on pressure transients and pipe strains is accurate, as demonstrated by the good agreement between computation and experiment.

•Wave interactions in plastically deforming piping can cause cavitation at unexpected times and locations in the system.

•A one-dimensional computational model for the effect of an elbow on pulse propagation is feasible, at least for the elbow geometry used in the SRI experiments.

•The effect of elbow curvature on pulse propagation is negligible, except perhaps right at the elbow; however, the effect of plastic deformation on the pulse may be masking the effect of elbow curvature.

REFERENCES

1 Florence, A. L. and Abrahamson, G. R., "Simulation of a Hypothetical Core Disruptive Accident in a Fast Flux Test Facility", HEDL-SRI-1, May 1973.

2 Fox, G. L., Jr. and Stepnewski, D. D., "Pressure Wave Transmission in a Fluid Contained in a Plastically Deforming Pipe", Trans. ASME, J. Pressure Vessel Technol., Vol. 96, No. 4, Nov. 1974, pp. 258-262.

3 Youngdahl, C. K. and Kot, C. A., "Effect of Plastic Deformation of Piping on Fluid-Transient Propagation", Nucl. Eng. Des., Vol. 35, 1975, pp. 315-325.

4 Romander, C. M. and Cagliostro, D. J., "Experiments on the Response of Flexible Piping Systems to Internal Pressure Pulses", Stanford Research Institute Project PYD-1960, Fourth Interim Report, April 1976.

5 Streeter, V. L. and Wylie, E. B., Hydraulic Transients, McGraw-Hill, New York, 1967.

6 Youngdahl, C. K. and Kot, C. A., "PTA-1: A Computer Program for Analysis of Pressure Transients in Hydraulic Networks, Including the Effect of Pipe Plasticity", ANL-76-64, November 1976.